Robotica (1998) volume 16, pp. 159–170. Printed in the United Kingdom © 1998 Cambridge University Press

Autonomous vehicle parallel parking design using function fitting approaches

Yongji Wang* and M.P. Cartmell†

(Received in Final Form: June 9, 1997)

SUMMARY

One of the most fundamental problems in the development of an intelligent highway system or an autonomous mobile robot system for factory use is to find the necessary input control variables for smooth and safe movement of the vehicle, or robot, between any two configurations. In this paper it is demonstrated that this problem can be converted into one of finding a fitting function which satisfies the boundary conditions. Three curves, a quintic polynomial, a cubic polynomial and a triangular function are developed to perform the *parallel transfer manoeuvre* which forms the basis of several important manoeuvres such as reverse parking, moving off, negotiating a stationary obstacle, overtaking a moving vehicle, and changing lane. A detailed discussion of the effect of the vehicle's steering angle limit on the feasibility of these manoeuvres is presented. Simulation results using three typical vehicles, a long commercial vehicle, an ordinary car, and a small laboratory robot, travelling along three curves are also presented and discussed. Based on the comparative study, some suggestions for further work are made. Compared with other methods, this approach is simple and provides excellent simulation of human driver techniques. The paper concludes with a focused discussion about the intergration of these techniques with satellite based GPS systems for automated vehicle guidance on highways.

KEYWORDS: Intelligent highway systems; Mobile robots; Autonomous vehicle; Trajectory generation; Collision avoidance; GPS system.

1. INTRODUCTION

It is generally accepted that a mobile robot, or steered vehicle, is a typical example of a nonholonomic system, and that all such applications are inherently difficult to work with.[1–9] In recent years, a considerable amount of work on the nonholonomic motion planning problem has been carried out and reported in the literature.[3,6,10–19] This problem can be described as one in which two arbitrary configurations of a system with nonholonomic constraints are given and the requirement is therefore to find the input control variables which satisfy the nonholonomic constraints so that the system can be driven from one configuration to the other. This problem is also referred to as one dealing with *the controllability of the nonholonomic system.*[20,21] Fuzzy logic concepts have also been used successfully in the simulation of the control of the reversing of trailer-truck vehicles.[22,23] Different mathematical tools have been used for solving the nonholonomic motion problem, and nonholonomic motion planning for a disk rolling on a plane was first studied by Li & Canny[12] using Stroke's theorem, and then later it was studied by Mukherjee & Anderson[5] using a surface integral approach. In Bushnell, Murray & Sastry, and Tilbury[3,6,24] the system is first converted into a chained form and then non-linear control theory and Lie algebra is used. Bushnell[3] give a comprehensive review of the work carried out using these methods. Recently the general property of the differential flatness of a system has been investigated and used,[14,25–28] however in this paper a different method is developed using the function fitting approach. In the approaches[3,5,6,24] the forms of the input variables are initially assumed as sinusoidal, polynomial, or piecewise constant functions in the time domain which are then integrated as a chained-form system to determine the unknown coefficients. The principal disadvantages of such an approach are that the shape of the generated path is difficult to control and it is difficult to control the relative position of the robot with respect to potential obstacles for collision avoidance. In addition this strategy is necessarily more complicated compared with the method presented in this paper.

The principal concept behind the method discussed in this paper is the attempted planning of a geometrical path $y = f(x)$ which satisfies boundary requirements. This is achievable because the requirements of the orientation angle and steering angle of the robot vehicle at initial and final configurations can be converted into the requirements of the first and second derivatives of the curve $y = f(x)$. The fact that the inputs may be expressed as functions of this path means that the method is simple and straightforward, and does not require that the motion from the initial configuraion to the final one must be completed in a pre-specified time T. This is not realistic in most cases anyway. The speed of the robot vehicle can be adjusted according to the prevailing road conditions, a feature consistent with human driver behaviour, and one which will be of particular importance for planned future integration of this work with global journey control concepts.

* Department of Computing & Electrical Engineering, Heriot-Watt University, Edinburgh, EH14 4AS (United Kingdom).
† Department of Mechanical Engineering, University of Edinburgh, King's Buildings, Mayfield Road, Edinburgh, EH9 3JL (United Kingdom).

In the case of a car-like robot moving on a plane its spatial location can be represented by three parameters, i.e. the two dimensional position of a reference point and an orientation angle. The required behaviour of the robot is to move from one specified global position and orientation (configuration) to another. This paper illustrates how the definitive nonholonomic motion planning problem for this scenario can be converted into a function fitting problem consistent with the trajectory generation problem for manipulators. The generated curves have geometrically simple, closed-form, expressions that precisely match the boundary conditions at the initial and final configurations on the paths. Another advantage of taking this approach is the wealth of appropriate tools available for the sort of numerical analysis required,[29] with the attendant advantage that clear physical insight into the problem is easily achieved.

One of the most obvious applications of wheeled robot motion control is in the development of an intelligent automated control system for highway vehicles, and a very considerable literature is devoted to this particular application area.[30–37]

The theme of the Intelligent Vehicle Highway System (IVHS) unites and integrates all the disparate research in this field, and particular attention has been paid by many of the researchers noted above to the sub-area of Automated Highway System (AHS). One of the most notable AHS projects has been the PATH programme based at the University of California at Berkeley.

This programme was motivated by the perceived need for increased highway capacity, and also by the general trend towards safety related practices (for example, a pertinent statistic according to Hedrick et al.[30] states that human error has been found to account for 90% of road accidents, thus strongly implying that robust and intelligent sensing and control systems could improve this situation considerably). The PATH programme considered multiple vehicle 'platoons' and identified three principal control tasks, (1) the assignation of a path for each vehicle, (2) the safe manoeuvring of the platoon formation, and (3) the implementation of these manoeuvres via feedback laws controlling throttle, braking, and steering actuators in each individual vehicle. Control strategies appear to have been predominantly analytical and have included the use of bespoke (smoothed) sliding mode control for the platoon formations as well as relatively simple classical compensators. At the end of this current paper an alternative overall strategy for sensing and control is overviewed. It should also be stated at this point that, in fact, relatively little attention has been paid to the problem of detailed planning of typical everyday vehicle manoeuvres (noting, however, the work done in[38–41]), and that therefore this paper is primarily reporting on an attempt to develop an entirely new and practical algorithm for path planning taking the physical limitations of the vehicle into account and the intentional simulation of a human driver's behaviour. As an example of the proposed function fitting approaches, a detailed discussion of the crucial parallel transfer manoeuver is examined in detail, and this is then followed by a more general discussion of proposals for the integration of function fitting planning procedures within a new global and local sensing and control strategy.

2. CONVERTING NONHOLONOMIC MOTION PLANNING INTO FUNCTION FITTING

In the following development the case when a variable, say y, is differentially expressed in terms of time t is represented by $\dot{y}$ and $\ddot{y}$ to denote $\frac{dy}{dt}$ and $\frac{d^2y}{dt^2}$; and when it is differentially expressed in terms of x, the following representations are used, y' and y'' denoting $\frac{dy}{dx}$ and $\frac{d^2y}{dx^2}$ respectively.

For a car-like robot as shown in Figure 1 (described henceforth as a 'robot', but on the understanding that it has the physical characteristics of a wheeled road vehicle), the nonholonomic kinematic constraint can be described as[42]

$$\dot{x}\cos\theta - \dot{y}\sin\theta = 0 \tag{1}$$

where (x, y, θ) represent the positon of the middle point of the rear axle, and the orientation angle of the robot body with respect to the horizontal, respectively. The configuration of the car-like robot is described by (x, y, θ, φ), where φ is the steering angle with respect to the robot body. The control inputs which drive the robot between configurations are chosen as the velocity of the middle point of the rear axle, u_1, and the steering velocity of the front steering wheel, $u_2 = \dot{\varphi}$. In this case, the purpose of the nonholonomic motion planning is to find u_1 and u_2, which satisfy the constraint of equation (1) and which can automatically drive the car-like robot from any arbitrary initial configuration $x_i, y_i, \theta_i, \varphi_i$ to a given final configuraion $x_f, y_f, \theta_f, \varphi_f$.

Equation (1) can be rewritten as

$$y' = \frac{dy}{dx} = \frac{\dot{y}}{\dot{x}} = \tan\theta \tag{2}$$

From Figure 1, it can be seen that the steering angle can be expressed as

$$\varphi = \arctan(L/R) \tag{3}$$

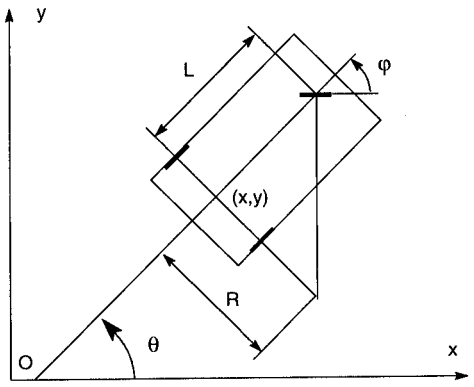

Fig. 1. A car-like robot. The configuration is represented by the position (x, y) of the midpoint of the rear axle and the orientation angle θ of the robot.

https://doi.org/10.1017/S0263574798000496 Published online by Cambridge University Press

where L is the wheelbase of the robot; and R represents the radius of the instantaneous rotation of middle point of the rear axle and can be expressed by a geometric curve in the form of $y = f(x)$ or by a parametric curve in the form of $x = x(t)$, $y = y(t)$.

$$R = \frac{(1 + y'^2)^{3/2}}{y''} = \frac{(\dot{x}^2 + \dot{y}^2)^{3/2}}{\dot{x}\ddot{y} - \dot{y}\ddot{x}} \tag{4}$$

From equations (3) and (4), we can obtain

$$y'' = \frac{\tan \varphi}{L}(1 + y'^2)^{3/2} \tag{5}$$

Obviously, from equations (2) and (5) we can see that the initial and final configuration requirements are equivalent to the following boundary conditions for a geometric curve $y = f(x)$

$$\begin{aligned} &y = y_i, \quad y_i' = \tan \theta_i, \quad y_i'' = \frac{\tan \varphi_i}{L(\cos \theta_i)^3} \quad \text{at } x = x_i \\ &y = y_f, \quad y_f' = \tan \theta_f, \quad y_f'' = \frac{\tan \varphi_f}{L(\cos \theta_f)^3} \quad \text{at } x = x_f \end{aligned} \tag{6}$$

In this case, the nonholonomic motion planning problem can be converted into the problem of finding a curve $y = f(x)$ which satisfies equation (1) and the boundary conditions in equations (6).

Once a reference path $y = f(x)$ has been generated it can be followed by a robot at different speeds according to the traffic congestion on the road. Adjusting speed is equivalent to adjusting $x = x(t)$. If $x = x(t)$ is known, then it follows that

$$\begin{aligned} x &= x(t) \\ y &= f(x(t)) \end{aligned} \tag{7}$$

Because both of the two control inputs $u_1 = \sqrt{\dot{x}^2 + \dot{y}^2}$ and $u_2 = \dot{\varphi}$ are functions of $x(t)$ and $y(t)$, they can be calculated from equations (3), (4) and (7) above.

There is also an alternative way of dealing with the initial and final steering angle reqirements. When a robot is moving, steering angle continuity along a path is always required for a smooth transition. However, if the robot does not move, the steering angle may be discontinuous, and this is a special case. This special case is considered by supposing that the steering angle of the robot can be manipulated without changing its initial and final positions and orientation angles (just like the reverse parking manoeuvring required by a car in a narrow space), then the configuration of the robot is represented by (x, y, θ) rather than (x, y, θ, φ). The initial and final configuration requirements are equivalent to the following boundary conditions

$$\begin{aligned} &y = y_i \quad \text{and} \quad y_i' = \tan \theta_i \quad \text{at } x = x_i \\ &y = y_f \quad \text{and} \quad y_f' = \tan \theta_f \quad \text{at } x = x_f \end{aligned} \tag{8}$$

A curve that satisfies equation (8) is sufficient for use as a path for driving the robot from the initial configuration to the final configuration. The extra requirement is that the steering angles at both terminals must be adjusted according to equation (3) without moving.

The following remarks are intended to assist in understanding this conversion and also the significance of designing a curve of the form $y = f(x)$. A geometric curve $y = f(x)$ in the plane is called a path. A trajectory is defined as the time course along such a path. Corresponding to the path, there exist different time courses.

If there is no velocity requirement at the initial and final configurations, then any trajectory along a planned path is satisfied. This means that $x = x(t)$ can be arbitrarily specified. Otherwise, we can adjust $x = x(t)$ to meet the velocity and acceleration requirements. Highway design is based on specifying a path rather than a trajectory as shown in Wang et al,[8] Wang,[18] and Wang & Linnett.[41] The speed of the vehicle is adjusted according to road congestion rather than at the road design stage.

3. FITTING FUNCTIONS

There are a number of curves which can be used for generating a path between two configurations. However, a satisfactory curve should meet some special requirements. Generally speaking, it should be

- computationally simple
- easy to satisfy the steering angle limit
- reasonably short
- able to demonstrate few undesirable oscillations.

In this section, three fitting curves are developed. All of them have closed form expressions that match precisely *a priori* the boundary conditions and also meet the above specifications.

3.1 Quintic polynomial

For satisfying the boundary conditions of equations (6), a curve with six undetermined parameters is requried. Obviously, a quintic polynomial can be used for this purpose, and the general expression for a quintic polynomial satisfying the constraints of equations (6) can be written in the form

$$y = \sum_{j=0}^{5} c_j x^j \tag{9}$$

The coefficients of c_j can be expressed as the following matrix form

$$C = T^{-1}A \tag{10}$$

where $C = [c_0 \ c_1 \ c_2 \ c_3 \ c_4 \ c_5]^T$, $A = [y_i \ y_f \ y_i' \ y_f' \ y_i'' \ y_f'']^T$ and

$$T = \begin{bmatrix} 1 & x_i & x_i^2 & x_i^3 & x_i^4 & x_i^5 \\ 1 & x_f & x_f^2 & x_f^3 & x_f^4 & x_f^5 \\ 0 & 1 & 2x_i & 3x_i^2 & 4x_i^3 & 5x_i^4 \\ 0 & 1 & 2x_f & 3x_f^2 & 4x_f^3 & 5x_f^4 \\ 0 & 0 & 2 & 6x_i & 12x_i^2 & 20x_i^3 \\ 0 & 0 & 2 & 6x_f & 12x_f^2 & 20x_f^3 \end{bmatrix}$$

https://doi.org/10.1017/S0263574798000496 Published online by Cambridge University Press

It is obvious that when the condition $x_i = x_f$ holds the matrix **T** becomes singular for any parameterisation. This problem arises from the choice of the reference frame but can be easily overcome by a proper rotational transformation of the co-ordinate frame if $y_i \neq y_f$ (meaning that the two points are not the same). In the case of $y_i = y_f$ (meaning that the two points coincide), a third configuration away from the initial and final ones must be chosen as a transitional configuration. The nonholonomic motion planning can be achieved by first driving the robot from the initial configuration to the transitional configuration, and then from the transitional configuration to the final configuration.

3.2 Cubic polynomial

If the boundary conditions are represented in the form of equations (8), then a curve with four undetermined parameters is needed. A cubic polynomial can be used for this purpose and the cubic polynomial satisfying the constraints of equations (8) can be written in the following form[29]

$$\begin{aligned} y = {} & y_i c^2 (x - x_f)^2 [1 + 2c(x - x_i)] \\ & + y_f c^2 (x - x_i)^2 [1 - 2c(x - x_f)] \\ & + y_i' c^2 (x - x_i)(x - x_f)^2 + y_f' c^2 (x - x_i)^2 (x - x_f) \end{aligned} \quad (11)$$

where $c = 1/(x_f - x_i)$.

The advantage of the latter strategy (equation (11)) over the former (defined in equation (9)) is that it has the potential for avoiding undesirable oscillations caused by the extra boundary conditions introduced by the steering angle requirement. However, its disadvantage is that the steering angle needed at each of the both configurations may be discontinuous.

3.3 Triangular function

A triangular function has the following general form

$$y = a \cdot \cos(\omega t + \psi) + b \quad (12)$$

where a, b, ω, and ψ are four undetermined parameters. If it is used to fit two configurations, only the boundary requirements of the position and the first order derivative for the curve can be specified at both ends.

Therefore, similar to the cubic polynomial function, it is only suitable for special manoeuvres where the steering angle at both the initial and final configuraions can be adjusted without changing the orientation of the robot. This curve is used later for performing the reverse parallel parking manoeuvre and its performance is compared with that of the other two curves.

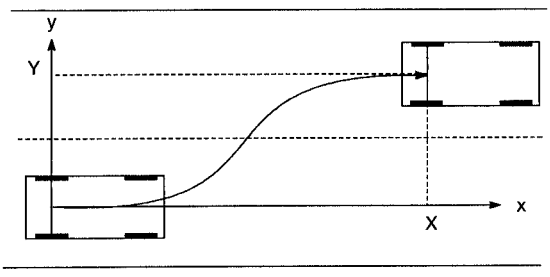

Fig. 2. Illustration of a parallel transfer manoeuvre.

4. MOTION ANALYSIS OF TYPICAL MANOEUVRES

4.1 Parallel transfer manoeuvres

Curves that produce a transition between parallel lines in the same direction are usually called *dog-leg* or *parallel transfer manoeuvres,* as shown in Figure 2. For simplicity, and without losing generality, the origin of the co-ordinate frame is chosen at the start point, with the positive x-axis being in the direction of the manoeuvre. A curve with this feature is of considerable use in performing a number of crucially important and fundamental manoeuvres such as moving off from behind a parked car, pulling up at the side of the road, changing lanes, reverse parking into a space between two parked cars, moving out to pass a stationary obstacle, overtaking a moving obstacle (a car or a truck), and parallel parking for adjusting a car's lateral position. All of these manoeuvres can be achieved using the basic parallel transfer manoeuvre, or alternatively a combiantion of two parallel transfers. In this section the three aforementioned fitting curves are used to plan the execution of the manoeuvre.

The requirements of the initial and final configurations for the manoeuvre are that at both ends the heading alignments of the robot are parallel to the x axis and the required steering angles are zero. From equations (6) it can be seen that these requirements are equivalent to

$$\begin{aligned} & y_i = 0, \quad y_i' = 0, \quad y_i'' = 0 \quad \text{at } x_i = 0 \\ & y_f = Y, \quad y_f' = 0, \quad y_f'' = 0 \quad \text{at } x_f = X \end{aligned} \quad (13)$$

where X and Y are the length and width of the manoeuvre respectively, as shown in Figure 2.

A single quintic polynomial fitting can be used for fitting. From equations (9) and (10) the quintic polynomial curve satisfying equation (13) has only three nonzero coefficients and can be written in the form

$$y = Y[10(x/X)^3 - 15(x/X)^4 + 6(x/X)^5] \quad (14)$$

If there is no steering angle requirement at both terminals, then the initial and final configurations can be described as

$$\begin{aligned} & y_i = 0, \quad y_i' = 0 \quad \text{at } x_i = 0 \\ & y_f = 0, \quad y_f' = 0 \quad \text{at } x_f = X \end{aligned} \quad (15)$$

in this case, the cubic polynomial satisfying equations (15) can be written as

$$y = Y[3(x/X)^2 - 2(x/X)^3] \quad (16)$$

If the triangular function is used for generating the curve satisfying equations (15), it has the following form

$$y = \frac{Y}{2}\left[1 - \cos\frac{x}{X}\pi\right] \quad (17)$$

Typical curves for simulating the transfer manoeuvres with $X = 6$ and $Y = 2.4$ are shown in Figure 3 and are all

https://doi.org/10.1017/S0263574798000496 Published online by Cambridge University Press

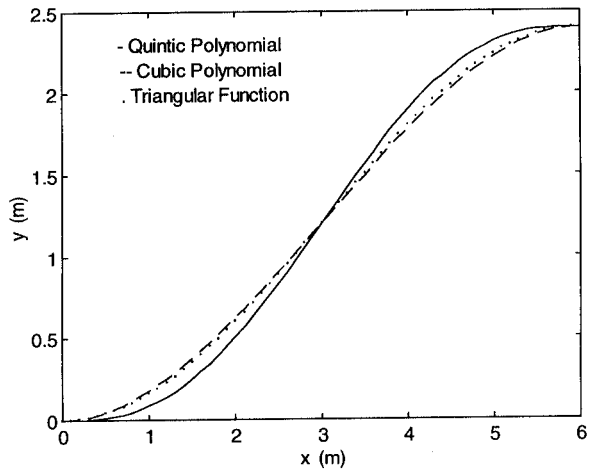

Fig. 3. Three curves for performing the parallel transfer manoeuvre. $X = 6$ and $Y = 2.4$.

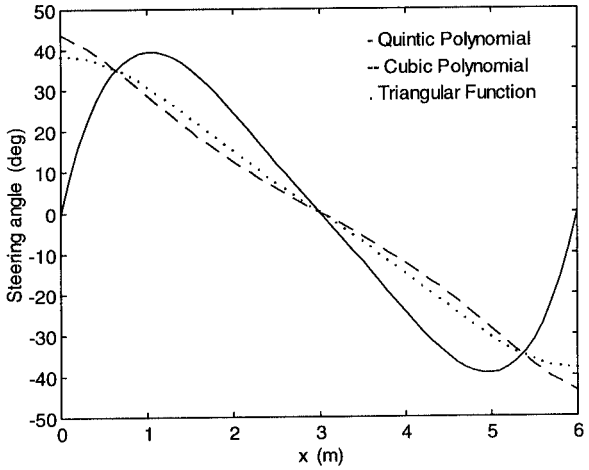

Fig. 5. The steering angles needed for a car with $L = 2.4$ to travel along the three curves given in Figure 3, $X = 6$ and $Y = 2.4$.

smooth and symmetric. In this case the curves for the cubic polynomial and the triangular function are indistinguishable from each other, however it is shown later that the latter is actually better than the former for this manoeuvre. The heading change of the robot versus the passed x is plotted in Figure 4 showing smooth characteristics in all three cases. The corresponding steering angles needed for a car with $L = 2.4$ to travel along them are plotted in Figure 5.

4.2 Steering angle limit and the minimum transfer length $X_{\min}$

Steering angle limit is an intrinsic feature of a car-like robot and it determines the critical conditions for distinguishing a feasible motion from an unfeasible one. The limited steering angle can be expressed by the following inequality constraint

$$-\varphi_{\max} \leq \varphi \leq \varphi_{\max} \tag{18}$$

where $\varphi_{\max}$ is a positive constant and represents the maximum deviation of the steering wheel from the heading of the robot. Due to the existence of the steering angle limit not every curve which satisfies the boundary conditions is therefore actually feasible. If the maximum steering angle of Figure 5 (as a case in point) exceeds the steering angle limit, then the curve is clearly unfeasible. Further, if a curve is unfeasible changing speed will have no effect on its feasibility. This is an intrinsic feature caused by the nonholonomic constraint. In such circumstances the remedy is to search for another curve which *is* feasible. In the remainder of this section the effect of steering angle limit on both X and Y is discussed in order to determine the minimum X corresponding to the maximum steering angle for a given Y.

In the following analysis, three hypothetical 'typical' vehicles are used, as shown in Figure 6. The first is a commercial vehicle representing the *long vehicle* type. The second is an ordinary car defining the *medium sized vehicle,* and the third is a small robot intended for laboratory use. Their dimensions are given in Table I. The steering angle limit used for each of them is 40°.

For a curve $y = f(x)$, equation (3) indicates that the maximum steering angle corresponds to the minimum radius of the instantaneous rotation, R, which occurs when $dR/dx = 0$, i.e. when the following condition is satisfied

$$y'''(1 + y'^2) - 3y'y''^2 = 0 \tag{19}$$

Differentiating the quintic polynomial given in equation (14) to obtain both y' and y'', and then

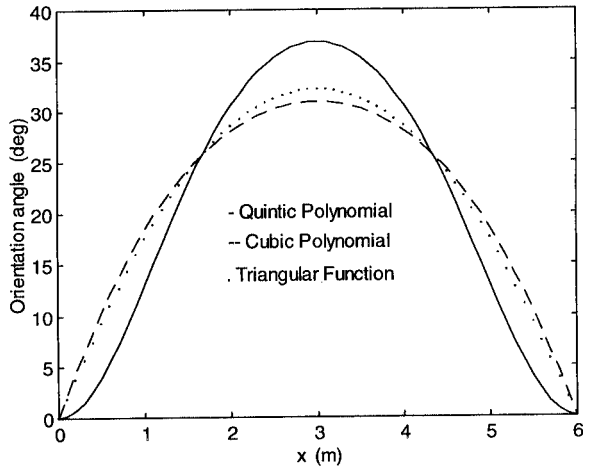

Fig. 4. Heading change of a robot travelling along the three curves given in Figure 3, $X = 6$ and $Y = 2.4$.

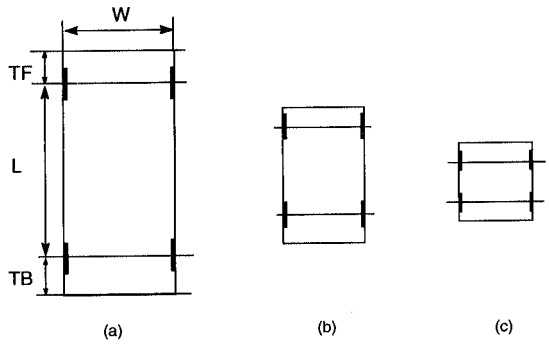

Fig. 6. Three typical vehicles: (a) a commercial rigid vehicle (b) an ordinary car (c) a laboratory robot.

https://doi.org/10.1017/S0263574798000496 Published online by Cambridge University Press

Table I. Dimensions of the three typical vehicles and the R_{min}, X_{min}, $\Delta x1_{max}$, $\Delta x2_{min}$ and $\Delta x3_{min}$ corresponding to the given Y and maximum steering angle φ_{max} for three different fitting curves:[a] quintic polynomial,[b] cubic polynomial,[c] triangular function. (a) A commercial rigid vehicle (b) an ordinary car (c) a laboratory robot.

Dimensions (meter)	(a)	(b)	(c)
W (body width)	2.5	1.6	1.5
TF (front overhand)	1.3	0.6	0.2
L (wheelbase)	6.2	2.4	1.1
TB (rear overhang)	2.5	0.8	0.2
TL (total length)	10	3.8	1.5
φ_{max}	40°	40°	40°
R_{min}	7.39	2.38	1.31
Y	3.5	2.4	2.0
X_{min}	11.86,[a] 12.46,[b] 11.37[c]	6.00,[a] 6.42,[b] 5.82[c]	3.58,[a] 3.97,[b] 3.60[c]
$\Delta x1_{max}$	1.41,[a] 2.14,[b] 1.32[c]	1.27,[a] 1.72,[b] 1.31[c]	0.80,[a] 0.96,[b] 0.79[c]
$\Delta x2_{min}$	12.95,[a] 12.82,[b] 12.55[c]	5.53,[a] 5.50,[b] 5.31[c]	2.98,[a] 3.21,[b] 3.01[c]
$\Delta x3_{min}$	2.95,[a] 2.82,[b] 2.55[c]	1.73,[a] 1.70,[b] 1.51[c]	1.48,[a] 1.71,[b] 1.51[c]

substituting them into equation (19), and simplifying, leads to

$$k_2 = \frac{30(1-k_1)^2 k_1^2 \sqrt{18k_1^2 - 18k_1 + 5}}{\sqrt{6k_1^2 - 6k_1 + 1}} \tag{20}$$

where $k_1 = x/X$ and $k_2 = X/Y$.

Equation (20) effectively indicates that when k_2 is fixed, the minimum value of R occurs at a fixed k_1. The relationship between k_1 and k_2 is plitted in Figure 7 and it can be seen that k_1 always falls into the range $0 \le k_1 \le 0.211$ or $0.789 \le k_1 \le 1$. In the range $0 \le k_1 \le 0.211$, the bigger the k_1, the smaller the k_2, however in the range $0.789 \le k_1 \le 1$, the bigger the k_1, the bigger the k_2. This indicates that for performing this manoeuvre, the front wheel must be steered very quickly to reach its maximum steering angle.

In a practical implementation of the transfer manoeuvre for an autonomous robot, Y can be measured using sensors (e.g. an ultrasonic, vision, or fused system). For example, for a lane change manoeuvre, Y is determined by the width of the lane and usually chosen to be equal to the width of one lane (from the centre of one lane to that of the next lane) and X determines the maximum steering angle needed. The longer the X, the smaller the steering angle. Corresponding to the maximum steering angle φ_{max}, there is a minimum X which must also satisfy equation (3).

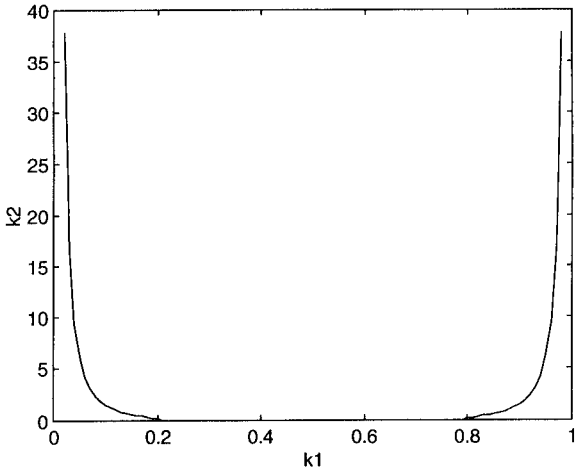

Fig. 7. Illustration of the relationship between k_1 and k_2.

Differentiating the quintic polynomial of equation (14) to obtain both y' and y'', and then substituting them into equation (3) leads to

$$\frac{LY}{\tan \varphi_{max}} = \frac{60k_1k_2^2(1 - 3k_1^2k_1^2)}{[1 + 900k_1^4k_2^2(1 - 2k_1 + 2k_2^2)^2]^{3/2}} \tag{21}$$

In this case equations (20) and (21) can be solved simultaneously to obtain the minimum X.

To summarise, for a given robot, L and φ_{max} are known, and therefore the general procedure for solving for the minimum X is as follows:

(1) Equation (20) is substituted into equation (21) to get an equation for k_1.
(2) This equation is solved for k_1.
(3) Equation (20) is used to obtain k_2 and then minimum $X = Yk_2$.

For the cubic polynomial given in equation (16), it can be proven that for any given X and Y, the maximum steering angle needed to follow this path occurs at both ends, i.e. $x = 0$ and $x = X$, and the relationship between the maximum steering and the X_{min} for a given Y is

$$X_{min} = \sqrt{\frac{6LY}{\tan \varphi_{max}}} \tag{22}$$

For the triangular function given in equation (17) it is also straightforward to prove that corresponding to any X and Y the maximum steering angle needed to follow this path occurs at both ends, i.e. at $x = 0$ and at $x = X$, and the relationship between the maximum steering and the X_{min} for a given Y is therefore

$$X_{min} = \pi \sqrt{\frac{LY}{2 \tan \varphi_{max}}} \tag{23}$$

The proof leading to equations (22) and (23) is omitted here for the sake of space, but it should be noted that these equations indicate that the bigger the width of the parked distance Y, or the effective wheelbase L, the

https://doi.org/10.1017/S0263574798000496 Published online by Cambridge University Press

bigger the X_{min}; and the bigger the steering angle limit, the smaller the X_{min}. This corresponds well to human driving experience. By comparing equations (22) and (23) it can be observed that for given Y, L and φ_{max}, the X_{min} for the triangular function is always smaller than that for the cubic polynomial. This means the triangular function is better than the cubic polynomial for manoeuvring in a narrow space. The simulation results for the X_{min}, using the three vehicles for the three curves, are given in Table I.

4.3 Reverse parking and moving off

A familiar example of the manoeuvring required by a robot or a human driver is parallel reverse parking, which is a special case of the parallel transfer manoeuvre discussed previously and shown in Figure 8. The goal is to move the robot into the space between two parked cars 1 and 2 (they may be two other obstacles). For a human driver, the strategy adopted for parallel reverse parking is to stop at the start position, and then to perform the following manipulations: to turn the steering wheels to the left limit, to reverse, straightening the wheels, to continue to reverse, turning the wheels to the other limit (still reversing), and then to straighten the wheels (noting that several iterations may be needed by a unskilled driver). When the reverse parking is complete, the robot adjusts its longitudinal position so as to be somewhere between the two parked vehicles.

All of the three curves can be used for this manoeuvre. The main potential problem is that collision between the moving robot vehicle and the parked cars may occur, and therefore two questions must be answered before implementing the three curves. The first is to determine the start position of the moving car relative to the parked car 1, and the second is to determine whether the length between the two parked cars is long enough to accommodate the moving car. Two parameters, $\Delta x1$ and $\Delta x2$, are introduced to describe the relative position of the start location of the moving car to the parked car 1 and that of the parked car 1 to car 2, respectively. $\Delta x1$ is defined as the offset of the origin of the co-ordinate frame Oxy from the rear edge of the car 1; and $\Delta x2$ is defined as the distance from the rear edge of the car 1 to the front edge of the car 2, as shown in Figure 8. $\Delta x2$ is the length of the space for parking the moving car. For a collision-free reverse manoeuvre it is obvious that there exists a maximum $\Delta x1$ and a minimum $\Delta x2$, denoted as $\Delta x1_{max}$ and $\Delta x2_{min}$ respectively. It is important to

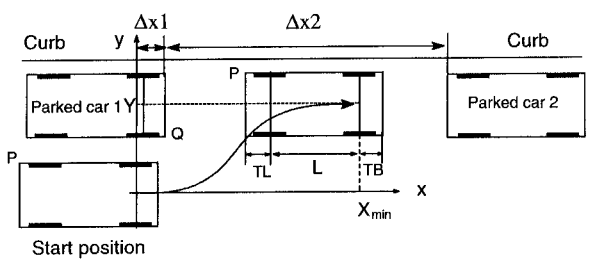

Fig. 8. Illustration of a reverse parking manoeuvre.

determine these two parameters because they describe the critical conditions for a successful reverse manoeuvre. As a curve is followed, $\Delta x1_{max}$ corresponds to the case where the front right corner P of the moving car just grazes the rear left corner Q of the parked car 1 (noting that $\Delta x1_{max}$ is the biggest distance allowable for collision free parking). In the following analysis simple geometry is used to establish a critical condition for determining $\Delta x1_{max}$ and $\Delta x2_{min}$.

If the path of the middle point of the rear axle is described in the form of $y = f(x)$, then the path travelled by P is geometrically related to the path $y = f(x)$ as follows

$$\begin{aligned} x_p &= -(TF + L)\cos\theta - 0.5W\sin\theta + x \\ y_p &= -(TF + L)\sin\theta + 0.5W\cos\theta + y, \quad x \in (0, X) \end{aligned} \tag{24}$$

where (x_p, y_p) are the co-ordinates of P, and TF and W represent the front overhang and the width o the moving vehicle respectively (see Figure 8).

The co-ordinates of point Q are represented by (refer again to Figure 8)

$$x_q = \Delta x1 \quad \text{and} \quad y_q = Y - 0.5W \tag{25}$$

The critical conditions for a collision-free manoeuvre between the moving car and car 1 are

$$x_q = x_p, \quad y_q = y_p \tag{26}$$

in this case $\Delta x1 = \Delta x1_{max}$. So from equations (24) and (25) we have

$$Y - 0.5W = -(TF + L)\sin\theta + 0.5W\cos\theta + y \tag{27}$$

$$\Delta x1_{max} = -(TF + L)\cos\theta - 0.5W\sin\theta + x \tag{28}$$

Note that y and θ are functions of x, so equation (27) contains only one unknown, x. Therefore, the procedure for solving $\Delta x1_{max}$ involves two steps:

(1) First solve equation (27) for x.
(2) Then substitute x into equation (28) to get $\Delta x1_{max}$.

In practice, the suggested start position $\Delta x1_{start}$ is

$$\Delta x1_{start} \le \Delta x1_{max} - 0.05 \tag{29}$$

where 0.05 is the minimum practically acceptable clearance between P and Q.

The distance, $\Delta x2$, between the two parked cars 1 and 2 should satisfy the following relation

$$\Delta x2 > X_{min} + TB - \Delta x1 \tag{30}$$

Corresponding to $\Delta x1_{start}$, the minimum distance between the two parked cars for a collision free reverse parking should be

$$\Delta x2_{min} = X_{min} + TB - \Delta x1_{max} - 0.05 \tag{31}$$

$\Delta x1_{max}$ and $\Delta x2_{min}$ for the three typical vehicles travelling along the three curves on a reverse parking manoeuvre are also shown in Table I.

From Table I we can conclude that from the viewpoint of the shortest $\Delta x2_{min}$ and the shortest X_{min}, the triangular function is the best choice for long and medium size vehicles for reverse parking. For the small

https://doi.org/10.1017/S0263574798000496 Published online by Cambridge University Press

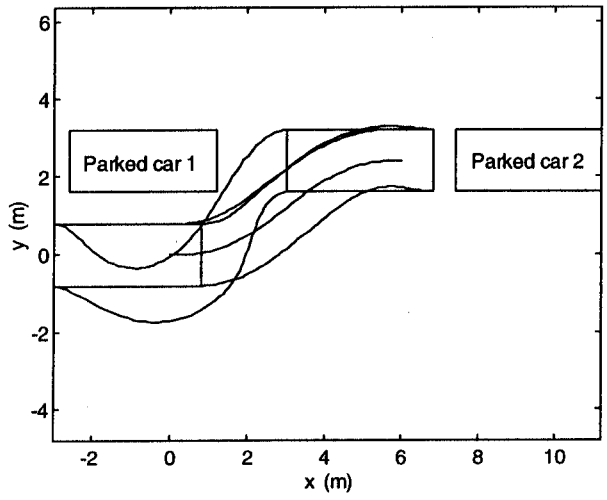

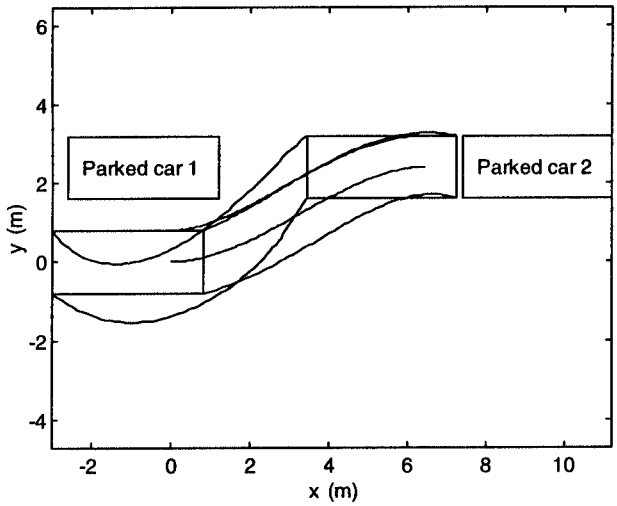

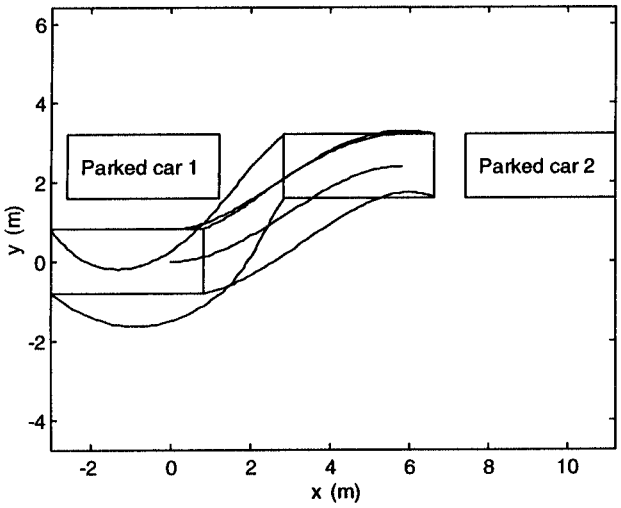

Fig. 9. Simulation results for reverse parking of an ordinary car. The common parameters used are: $Y = 2.4$, $\varphi_{max} = 40°$, $TF = 0.6$, $L = 2.4$, $TB = 0.8$, $W = 1.6$, $\Delta x1 = 1.2$, and $\Delta x2 = 6.2$. (a) Quintic polynomial, $X = 6.0$, (b) cubic polynomial, $X = 6.42$, (c) triangular function, $X = 5.82$.

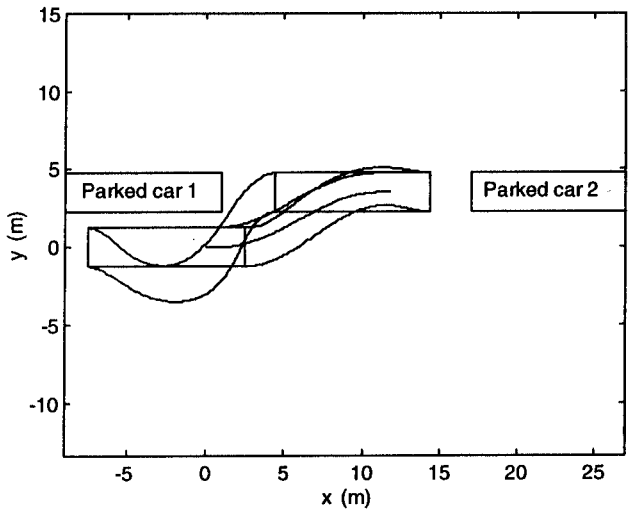

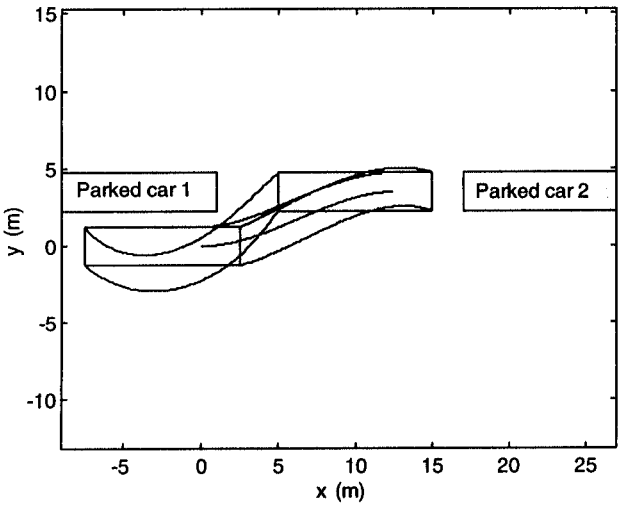

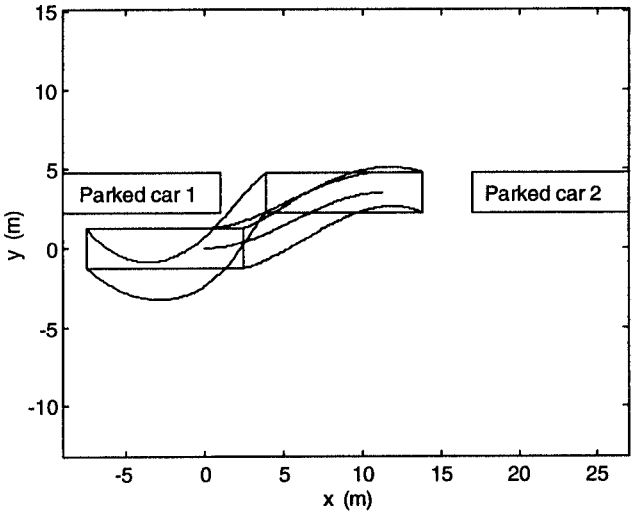

Fig. 10. Simulation results for reverse parking of a commercial vehicle. The common parameters used are: $Y = 3.5$, $\varphi_{max} = 40°$, $TF = 1.3$, $L = 6.2$ $TB = 2.5$, $W = 2.5$, $\Delta x1 = 1.0$, and $\Delta x2 = 16.0$. (a) Quintic polynomial, $X = 11.86$, (b) cubic polynomial, $X = 12.46$, (c) triangular function, $X = 11.37$.

https://doi.org/10.1017/S0263574798000496 Published online by Cambridge University Press

robot, the quintic polynomial is suggested because of its shortest $\Delta x2_{min}$, and shortest X_{min}, as well as its continuous steering angle at both ends.

Simulation results for a reverse parking manoeuvre for the ordinary car using the three curves are shown in Figure 9(a), (b), and (c), respectively. The common parameters used for the simulation are: $Y = 2.4$, $\varphi_{max} = 40°$, $TF = 0.6$, $L = 2.4$, $TB = 0.8$, $W = 1.6$, $\Delta x1 = 1.2$, and $\Delta x2 = 6.2$. The X values used in Figure 9(a), (b), and (c) are 6, 6.42, and 5.82, respectively. In each Figure, the locus of six points (the middle point of the rear axle, the contact point of the right rear wheel with the ground, and the four corners of the vehicle) is plotted.

By comparing Figures 9(a), 9(b), and 9(c), it can be observed that the parking distance $\Delta x2_{min}$ needed for the triangular function is the shortest; that the distance swept out by the front left corner of the moving vehicle in the y-direction for the quintic polynomial is the biggest; and finally that the cubic polynomial has the biggest start position $\Delta x1_{max}$.

Figures 10(a), 10(b), and 10(c) illustrate simulation results for the long commercial vehicle travelling along the three curves respectively. For this kind of vehicle it can be seen that the triangular function gives the shortest parking distance $\Delta x2_{min}$; that the cubic polynomial generates the shortest distance in the y-direction, and the quintic polynomial develops both the longest $\Delta x2_{min}$ and the longest distance in the y-direction.

In Figures 11(a), 11(b), and 11(c) simulation results are depicted for the small laboratory robot travelling along the three curves respectively. From the Figures we can see that because the distance swept by the curves in the y-direction is almost the same, the quintic polynomial is the best choice because of its shortest $\Delta x2_{min}$ as well as for reasons of steering angle continuity.

The start position for different kinds of vehicles and different kinds of curves is different in each case, and it is important that attention is paid to this issue, noting that the position is determined by equation (31). Perusal of Figures 9, 10, and 11, and Table I clearly illustrates the point.

In the case of a vehicle parked behind another vehicle, moving off is a typical manoeuvre for which the manipulation is just the reverse of the reverse parking procedure. The co-ordinate frame is chosen like that shown in Figure 12. In this case because of the requirement for continuous post-start motion only the quintic polynomial is suggested as being appropriate. The minimum distance between the two cars, $\Delta x3_{min}$, can be solved using a similar procedure to that for the reverse parking.

In fact, $\Delta x3_{min}$ is equal to

$$\Delta x3_{min} = \Delta x2_{min} - TL \tag{32}$$

where TL is the total length of the moving vehicle. $\Delta x3_{min}$ for each of the three vehicles travelling along the three curves respectively is also given in Table I.

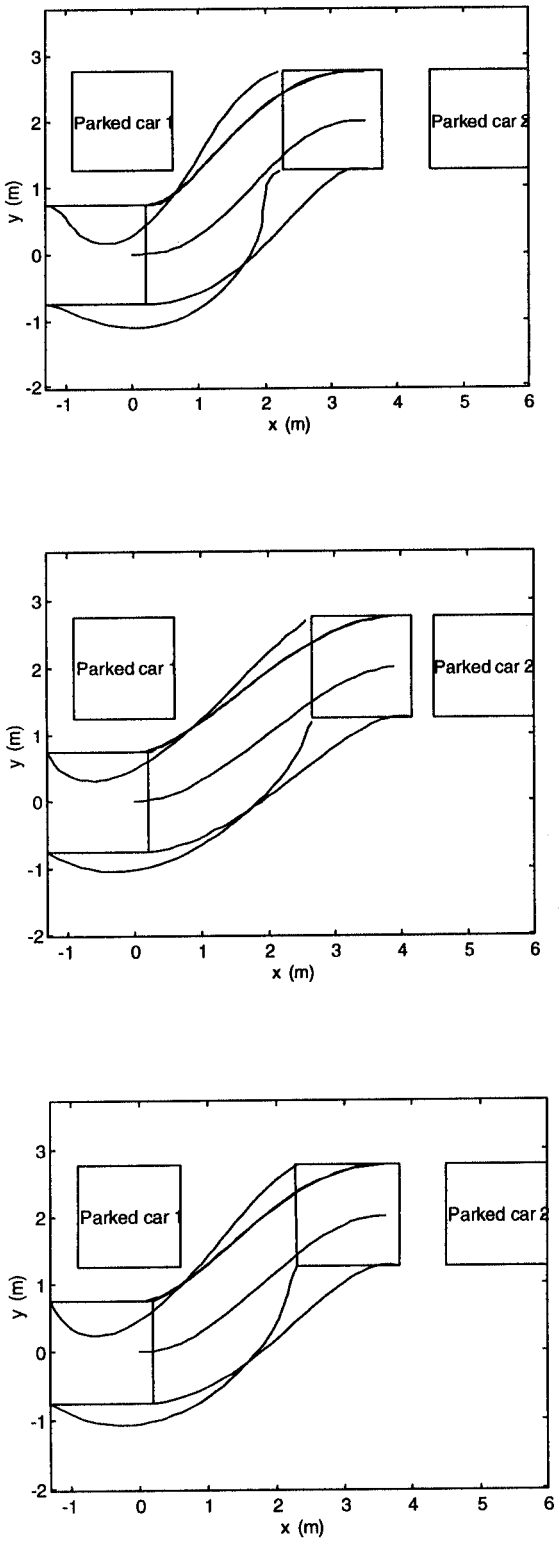

Fig. 11. Simulation results for reverse parking of a small laboratory robot. The common parameters used are: $Y = 2.0$, $\varphi_{max} = 40°$, $TF = 0.2$, $L = 1.1$, $TB = 0.2$, $W = 1.5$, $\Delta x1 = 0.6$, and $\Delta x2 = 3.9$. (a) Quintic polynomial, $X = 3.58$, (b) cubic polynomial, $X = 3.97$, (c) triangular function, $X = 3.60$.

4.4 Lane change, obstacle avoidance and parallel parking manoeuvres

The Lane Change manoeuvre is the simplest of all the parallel transfer manoeuvres, and is illustrated in Figure 2. In this case the road ahead is assumed to be clear, and

https://doi.org/10.1017/S0263574798000496 Published online by Cambridge University Press

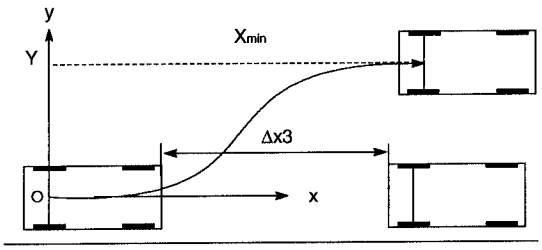

Fig. 12. Illustration of moving off from behind a parked vehicle.

obstacles. The only problem is to choose a proper length of X, according to the speed of the vehicle, in order to maintain a reasonably large minimum instantaneous radius R for the vehicle so that radial forces are kept to a minimum. Clearly, the higher the speed of the vehicle the smaller the corresponding value of X.

Figure 13 illustrates another common manoeuvre in the form of a moving vehicle pulling out to pass a stationary obstacle, or to overtake another moving vehicle, and in this paper both manoeuvres are generally regarded as *obstacle avoidance* manoeuvres.

If two parallel transfers are connected by a straight line, with the second parallel transfer curve being a reversed version of the first, then the vehicle can be made to transfer from one line to a parallel track, move forward for a while, and then return to the original line. Because passing, or overtraking, a vehicle occurs when the vehicle concerned is in motion, the steering angle must not be too large. Generally speaking, φ does not exceed 15°. Therefore the appropriate X value is generally long enough to avoid a collision between the vehicles during the first parallel transfer, and also to avoid cutting-in during the second parallel transfer.

The procedure for dealing with this manoeuvre is to use the suggested maximum steering angle (for example, 15°) and Y, L as known parameters in equations (20) and (21), then to determine X as the distance between the start position of the manoeuvre to the rear edge of the obstacle (stationary or moving vehicle) where the start point of the straight line is located. The length of the straight line may be chosen as that of the obstacle, so as a result of this the front edge of the obstacle is the start position and X is the length requied for the second transfer manoeuvre.

Figure 14 illustrates the sort of parallel parking manoeuvre which may be encountered in a parking lot,

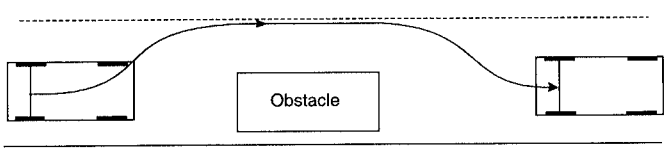

Fig. 13. Illustration of an obstacle avoidance manoeuvre. It includes moving out to pass a stationary vehicle or to overtake a moving vehicle.

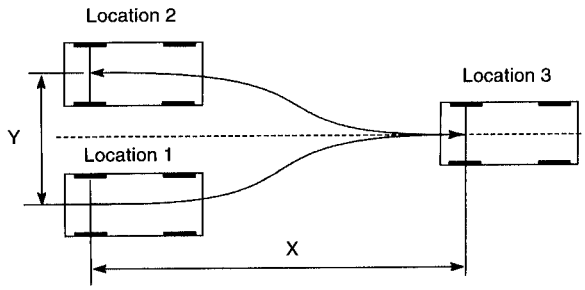

Fig. 14. Illustration of a parallel parking manoeuvre.

and it should be noted that it differs somewhat from the reverse parking manoeuvre. The vehicle is to be moved from location 1 to location 2, and it is certainly intuitively obvious that it is impossible to move directly from location 1 to location 2. This fact can also be proved using the nonholonomic constraint equation (1). A third location 3 must be chosen (noting that it may be in front of, or behind, the vehicle, depending on where there is a clear space). Obviously, the strategy used by a human driver in this case is that a forward parallel transfer is performed and then followed by a backward parallel transfer if the front space is clear. Note that these two manoeuvres may be not symmetric, and in some cases the backward manoeuvre may in fact simply be a straight line. Given L, Y, and φ_{max}, the X_{min} may be determined and used to assess whether there is enough space for this manoeuvre.

5. A SATELLITE GPS APPROACH TO VEHICLE GUIDANCE AND CONTROL

One of the distinct advantages of using satellite GPS receivers for fixing a moving location is that global coverage is wide and reliability is quite high (i.e. despite inevitable 'lost' signals modern GPS receivers can re-fix and re-calculate quickly enough to ensure a high continuity of information). The cost of a GPS receiver is closely linked to its performance with base-line fix accuracy down to around 300–100 m for basic equipment using degraded signals from the US Standard Positioning System, to sub-centimetre accuracy for Differential Carrier Phase systems. In the vehicle navigation application it is proposed that GPS navigation could be used to identify the optimal (ie shortest course) progression of a vehicle along a pre-determined electronically defined route. The pre-planned route is intended to be such that all the necessary map-dictated manoevre decision points are identified in advance. This part of the vehicle navigation problem is called the *global* part, and is intended to work in tandem with the *local* sensing and control strategy based on on-board sensors driving a function fitting local planner for direct control of the vehicle's actuators. This approach does not utilise the platooning concept since the local sensing required for the function fitting planner and controller would provide all the data needed to ensure that safe distances are continuously maintained. It is of course important to recognise that there have been many AHS projects and that considerable technology already exists to implement

https://doi.org/10.1017/S0263574798000496 Published online by Cambridge University Press

many of them (refer to Hedrick et al[30] for a comprehensive review of the California PATH programme, Kawashima[32] for a resume of the Japanese AMTICS and RACS experiments, and Catling & McQueen[33] for a discussion of various European demonstrator programmes such as DRIVE, PROMETHEUS, Autoguide (UK), and a selection of specific navigation and route guidance systems.

These systems mostly concentrate on roadside beacons or cellular radio for information retrieval or Road Transport Informatics (RTI)). Many of the results from the above projects in the areas of digital mapping and road databases are directly relevant to the current and future work overviewed here, and it is noted that satellite techniques did form part of one of the seven theme groups in the DRIVE project. However the integration of state of the art in differential carrier phase GPS with the function fitting techniques discussed in previous sections of this paper will continue to form the basis for original on-going research, and will exploit many of the findinngs of Cartmell et al[43] in parallel work on the control of mobile cranes.

6. CONCLUSIONS

In this paper, it has been shown that the so-called nonholonomic motion planning problem, i.e. the problem of finding the inputs needed to control a robot vehicle from a given initial configuration to a final configuration may be converted into that of finding a fitting function which satisfies the boundary conditions. Theoretically, any constructed curve that satisfies the boundary requirements is feasible. The difficulty is in finding a good curve which is able to simulate satisfactorily a human driver's behaviour, and meanwhile to meet the requirement of the steering angle limit. To this end three curves have been developed (a quintic polynomial, a cubic polynomial and a triangular function) for performing the parallel transfer manoeuvre which, as shown, is further used as the basis for reverse parking, overtaking, and other manoeuvres. A detailed discussion of the effect of the steering angle limit on the minimum length $X_{\min}$, on the choice of the start position of reverse parking, and on the minimum distance between two parked cars allowed for parking another vehicle has been presented, and the procedure for solving them has been given. The simulation results indicate that the approach is efficient and that the generated path is quite consistent with that followed by a practical vehicle used on modern roads. for the three proposed curves the following conclusions are suggested for different manoeuvres:

(1) To perform reverse parking the triangular function should be used for ordinary cars and long vehicles, and the quintic polynomial should be used for small robots.
(2) To perform other manoeuvres which require continuous steering control, the quintic polynomial can be successfully used for all three types of vehicle.

Immediate developments will focus on building up a library of simulation modules for all basic manoeuvres (including right turn, left turn, three point turn, and so on). The ultimate aim is to develop a practical function fitting based navigation system for intelligent highway systems integrated with current satellite GPS technologies for global navigation. Parallel developments using in-factory sonar and IR beacons for intelligent control of autonomous robots are also envisaged.

ACKNOWLEDGEMENTS

The financial support of the KC Wong Education Foundation, Hong Kong, is gratefully acknowledged, as is the use of computational facilities at Heriot-Watt University and the University of Edinburgh.

References

1. L. Dubins, "On curves of minimal length with a constraint on average curvature and with prescribed initial and terminal positions and tangents" *Amer. J. Mathematics* **79,** 497–516 (1957).
2. A.M. Bloch, M. Reyhanoglu and N.H. McClamroch, "Control and stabilisation of nonholonomid dynamic systems" *IEEE Trans. on Automatic control* **37,** 1746–1757 (1992).
3. L.G. Bushnell, D.M. Tilbury and S.S. Sastry, "Steering three-input nonholonomic systems: the fire truck example" *Int. J. Robotics Research* **14,** 366–381 (1995).
4. A. Cole, J. Hauser and S.S. Sastry, "Kinematics and control of a multifingered robot hand with rolling contact" *IEEE Trans. on Automatic Control* **34,** 398–404 (1989).
5. R. Mukherjee and D. Anderson, "A surface integral approach to the motion planning of nonholonomic systems" *ASME J. Dynamics systems, Measurement and Control* **116,** 315–325 (1994).
6. R.M. Murray and S.S. Sastry, "Nonholonomic motion planning: Steering using sinusoids" *IEEE Trans. on Automatic Control* **38,** 700–716 (1993).
7. M. Sampei, T. Tamura, T. Kobayashi and N. Shibui, "Arbitrary path tracking control of articulated vehicles using nonlinear control theory" *IEEE Trans. on Control Systems Technology* **3,** 125–131 (1995).
8. Y. Wang, J.A. Linnett and J.W. Roberts, "Motion feasibility of a wheeled vehicle with a steering angle limit" *Robotica* **12,** Part 3, 217–226 (1994).
9. Y. Wang, J.A. Linnett and J.W. Roberts, "Kinematics, kinematic constraints, and path planning for wheeled mobile robots" *Robotica* **12,** Part 5, 391–400 (1994).
10. S. Hirose, E.F. Fukushima and S. Tsukagoshi, "Basic steering control methods for the articulated body mobile robot" *IEEE Control Systems* **10,** 5–14 (1995).
11. S. Jagannathan, S.Q. Zhu and F.L. Lewis, "Path planning and control of a mobile base with nonholonomic constraints" *Robotica* **12,** Part 6, 529–539 (1994).
12. Z. Li and J. Canny, "Motion of two rigid bodies with rolling constraint" *IEEE Trans. on Robotics and Automation* **6,** 62–72 (1990).
13. R.M. Murray, "Non-linear control of mechanical systems: a Lagrangian perspective" *IFAC Symposium on Non-linear Control Systems Design (NOLCOS),* Lake Tahoe, CA, USA (1995) pp. 1–12.
14. R.M. Murray, "Applications and extensions of goursat normal form to control of non-linear systems" *Proc. IEEE Conference on Control and Decision,* Texas, (1993) pp. 3425–3430.
15. Y. Nakamura and R. Mukherjee, "Nonholonomic motion planning of space robots via a bi-directional approach" *IEEE Trans. on Robotics and Automation* **7,** 500–514

https://doi.org/10.1017/S0263574798000496 Published online by Cambridge University Press

16. M. Sayer, "Vehicle offtracking models" *Transportation Research Record 1052, Symposium on Geometric Design for Large Trucks,* Transportation Research Board, Washington, D.C. (1986) pp. 53–62.
17. B. Steer, "Trajectory planning for a mobile robot" *Int. J. of Robotics Research* **8,** 3–14 (1989).
18. Y. Wang, "Kinematics, motion analysis and path planning for four kinds of wheeled mobile robots" *PhD thesis* (Edinburgh University, Scotland, U.K., 1995).
19. Y. Wang, "Nonholonomic motion planning: a polynomial fitting approach" *Proc. IEEE Int. Conf. on Robotics and Automation,* Minnesota, USA (1996) pp. 2956–2961.
20. L. Laumond, "Controllability of a multibody mobile robot" *IEEE Trans. on Robotics and Automation* **9,** 755–763 (1993).
21. J. Laumond, P.E. Jacobs, M. Taix and R.M. Murray, "A motion planner for nonholonomic mobile robots" *IEEE Trans. on Robotics and Automation* **10,** 577–593 (1994).
22. S. Kong and B. Kosko, "Adaptive fuzzy systems for backing up a truck-and-trailer" *IEEE Trans. on Neural Networks* **3,** 211–223 (1992).
23. K. Tanaka and M. Sanabu, "A robust stabilization problem of fuzzy control systems and its application to backing up control of a truck-trailer" *IEEE Trans. on Fuzzy Systems* **2,** 119–134 (1994).
24. D. Tilbury, R.M. Murray and S.S. Sastry, "Trajectory generation for the N-trailer problem using the Goursat norm form" *IEEE Trans. on Automatic control* **40,** 802–819 (1995).
25. M. Fliess, J. Levine, P. Martin and P. Rouchon, "On differentially flat non-linear systems" *IFAC symposium on Non-linear Control Systems Design (NOLCOS),* Bordeaux, France (1992) pp. 408–412.
26. M. van Nieuwstadt, M. Rathinam and R.M. Murray, "Differential flatness and absolute equivalence" *Proc. IEEE Conference on Control and Decision,* Florida (1994) pp. 326–333.
27. P. Rouchen, M. Fliess, J. Levine and P. Martin, "Flatness and motion planning: the car with n trailers" *European Control Conference,* Groningen, The Netherlands (1992) pp. 1518–1522.
28. P. Rouchen, M. Fliess, J. Levine and P. Martin, "Flatness and defect of non-linear systems: introductory theory and examples" *Int. J. Control* **61,** 1327–1361 (1995).
29. I.D. Faux and M.J. Pratt, *Computational Geometry for Design and Manufacture* (John Wiley and Sons Limited, London, 1987).
30. J.K. Hedrick, M. Tomizuka and P. Varaiya, "Control issues in automated highway systems" *IEEE Control systems* **9,** 21–30 (1994).
31. D.H. Roper and G. Endo, "Advanced traffic management in California" *IEEE Trans. on Vehicular Technology* **40,** 152–158 (1991).
32. H. Kawashima, "Two major programs and demonstrations in Japan" *IEEE Trans. on Vehicular Technology* **40,** 141–146 (1991).
33. I. Catling and R. McQueen, "Road transport informatics in Europe – Major programs and demonstrations" *IEEE Trans. on Vehicular Tehcnology* **40,** 132–140 (1991).
34. S.E. Shladover, C.A. Desoer, J.K. Hedrick, M. Tomizuka, J. Walrand, W.-B. Zhang, D.H. McMahon, H. Peng, S. Sheikholeslam and N. McKeown, "Automatic vehicle control developments in the PATH program" *IEEE Trans. on Vehicular Technology* **40,** 114–130 (1991).
35. R.E. Fenton and R.J. Mayhan, "Automated highway studies at the Ohio State University – An overview" *IEEE Trans. on Vehicular Technology* **40,** 100–113 (1991).
36. R.E. Fenton, "IVHS/AHS: Driving into the future" *IEEE Control Systems* (December 13–20 1994).
37. J.G. Bender, "An overview of systems studies of automated highway systems" *IEEE Trans. on Vehicular Technology* **40,** 82–99 (1991).
38. Y. Kanayama and N. Miyake, "Trajectory generation for mobile robots" *The Third Int. Symposium on Robotics Research* (D. Fraugeras and G. Giralt, Eds.) (The MIT Press, Cambridge, 1986) pp. 333–340.
39. W.L. Nelson, "Continuous steering-function control of robot carts" *IEEE Trans. on Industrial Electronics* **36,** 330–337 (1989).
40. W.N. Patten, H. Wu and W. Cai, "Perfect parallel parking via Pontryagin's principle" *Trans. of ASME, J. of Dynamic systems, Measurement, and Control* **116,** 723–728 (1994).
41. Y. Wang and J.A. Linnett, "Vehicle kinematics and its application to highway design" *ASCE J. of Transportation Engineering* **121,** 63–74 (1995).
42. Y. Wang, J.A. Linnett and J.W. Roberts, "A unified approach to inverse and direct kinematics for four kinds of wheeled mobile robots and its applications" *Proc. IEEE Int. Conf. on Robotics and Automation,* Minnesota, USA (1996) pp. 3458–3465.
43. M.P. Cartmell, T.E. Alberts, L. Morrish and A.J. Taylor, "Controlling the nonlinear dynamics of gantry cranes" *Machine Vibration* **5,** 197–210 (1996).